AIP | Applied Physics Letters

Electro-optic polymer infiltrated silicon photonic crystal slot waveguide modulator with 23 dB slow light enhancement

Che-Yun Lin, Xiaolong Wang, Swapnajit Chakravarty, Beom Suk Lee, Weicheng Lai, Jingdong Luo, Alex K.-Y. Jen, and Ray T. Chen

Citation: Applied Physics Letters **97**, 093304 (2010); doi: 10.1063/1.3486225
View online: http://dx.doi.org/10.1063/1.3486225
View Table of Contents: http://scitation.aip.org/content/aip/journal/apl/97/9?ver=pdfcov
Published by the AIP Publishing

Electro-optic polymer infiltrated silicon photonic crystal slot waveguide modulator with 23 dB slow light enhancement

Che-Yun Lin,[1,a)] Xiaolong Wang,[2,b)] Swapnajit Chakravarty,[2] Beom Suk Lee,[1] Weicheng Lai,[1] Jingdong Luo,[3] Alex K.-Y. Jen,[3] and Ray T. Chen[1,c)]
[1]*Department of Electrical and Computer Engineering, University of Texas at Austin, Austin, Texas 78712, USA*
[2]*Omega Optics Inc., Austin, Texas 78759, USA*
[3]*Department of Materials Science and Engineering, University of Washington, Seattle, Washington 98195, USA*

(Received 27 June 2010; accepted 15 August 2010; published online 3 September 2010)

A silicon/organic hybrid modulator integrating photonic crystal (PC) waveguide, 75 nm slot, and electro-optic (EO) polymer is experimentally demonstrated. Slow light in PC waveguide and strong field confinement in slot waveguide enable ultraefficient EO modulation with a record-low $V_\pi \times L$ of 0.56 V mm and an in-device effective r_{33} of 132 pm/V. This result makes it the most efficient EO polymer modulator demonstrated to date. The modulated signal shows strong wavelength dependence and peak enhancement of 23 dB near the band edge of defect mode, which confirms the signature of the slow light effect. © *2010 American Institute of Physics*. [doi:10.1063/1.3486225]

Silicon has long been the optimal material for microelectronics. Building photonic devices in silicon bears the advantage of being compatible to complementary metal-oxide-semiconductor fabrication technology, which can lead to monolithic integration of microelectronic and photonic devices on a single silicon chip. However, due to its centrosymmetric crystal structure, silicon shows no Pockels effect. Electrically driven optical modulation in silicon photonic devices typically relies on free carrier injection[1] or depletion[2] where the achievable modulation bandwidth is limited by time constants related to removing or injecting free carriers to the modulation arm.

By contrast, EO polymers offer very high Pockels coefficient ($r_{33} > 300$ pm/V)[3] with extremely fast response speed in the terahertz range.[4] Ultrahigh bandwidth[5] and subvolt half-wave driving voltage (V_π)[6,7] have been demonstrated in EO polymer modulators. However, the size of these devices is limited by conventional waveguide structures with millimeter to center meter interaction length. Compared to conventional waveguides, silicon PC waveguide offers slow light-enhanced light-matter interaction, which can shrink the interaction length down to 80 μm[8] and a reduced index change of 4.2×10^{-3} to achieve switching in a silicon-based structure.[9] Photonic devices based on silicon/EO polymer hybrid material system combine strong optical confinement abilities of silicon with superior EO modulation efficiency of polymers. Compared with conventional EO polymer photonic devices, this hybrid approach requires no cladding polymer layers. This should lead to higher poling efficiency and lower driving voltage with fabrication simplicity. Slot waveguide infiltrated with EO polymers in Mach–Zehnder modulators (MZM) have reported half wave voltage of 0.25 V, and $V_\pi \times L$ of 5 V mm.[10] A more advanced design using silicon PC slot waveguide can exploit slow light effect from the defect mode close to the photonic band edge,[11] thus even lower $V_\pi \times L$ can be expected. Compared with PC devices without slot,[8,9] integrating EO polymer in slot PC waveguide offers better potential for high speed operation.[5] In this paper, we present the design and experimental demonstration of a MZM based on EO polymer infiltrated silicon PC slot waveguide with slow light enhanced EO modulation.

Figure 1(a) shows the schematic of the PC slot waveguide. Input and output waveguides are conventional silicon strip waveguide, which connect to PC slot waveguide with optical mode converter[12] for better mode-matching. The PC waveguide is a W1 waveguide formed by replacing a row of air holes with a narrow slot of width $w=75$ nm, which provides good optical confinement and modulation efficiency without compromising the feasibility of EO polymer infiltration. The modulation region, with slot nanostructures, is formed in a hexagonal lattice PC slab with lattice constant $a=385$ nm and hole diameter $d=217$ nm, which has a total length of 308 μm. Silicon PC regions including air holes and slot are fully covered by EO polymer with strong EO coefficient (AJ-CKL1/APC).[13] Refractive index of infiltrated polymer is 1.63 at 1.55 μm. Dispersion diagram of the guided mode is shown in Fig. 2(a), which is calculated by

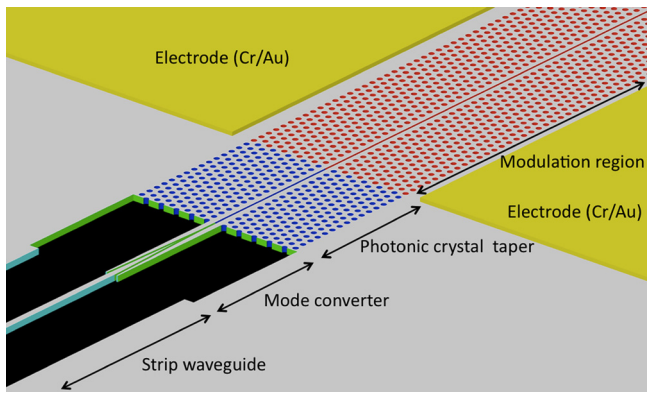

FIG. 1. (Color online) Schematic of the input strip waveguide, optical mode converter, PC taper, and modulation region.

a)Electronic mail: cheyunlin@gmail.com.
b)Electronic mail: alan.wang@omegaoptics.com.
c)Electronic mail: raychen@uts.cc.utexas.edu.

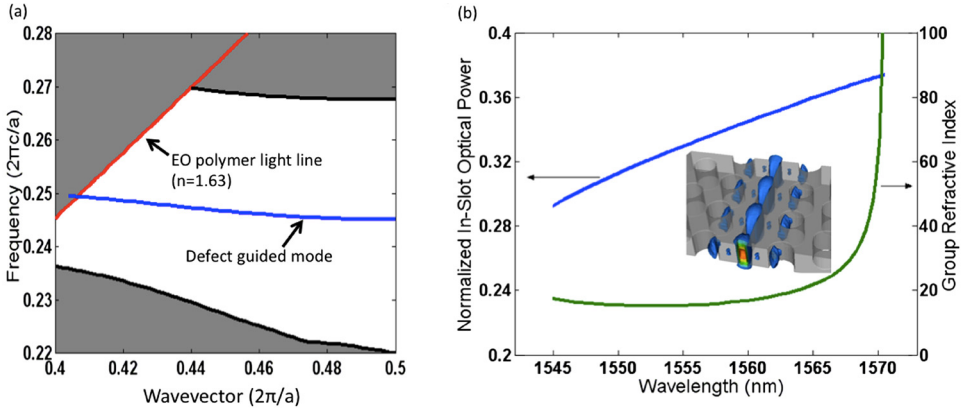

FIG. 2. (Color online) (a) Enlarged portion of the dispersion diagram for the guided mode. (b) Group index (n_g) and normalized in-slot optical power of the guided mode as a function of the optical wavelength. Optical mode profile at $n_g=100$ is shown in inset.

three-dimensional plane wave expansion (PWE) method. The group refractive index n_g of the guided mode as a function of wavelength is shown in Fig. 2(b), which shows that n_g can exceed 100 when the wavelength is tuned close to the band edge of 1569 nm. The optical intensity profile ($|E|^2$) of the guided mode at $n_g=100$ is shown in inset of Fig. 2(b). Figure 2(b) also shows in-slot optical power weight (Γ) in the total guided mode power. It should be noted that integration of 75 nm slot waveguide into photonic crystal (PC) waveguide causes light with low group velocity within the defect mode spectrum remain concentrated in the slot, which will otherwise penetrate to second or third row of holes without the presence of a slot.[14] With lightly doped silicon functioning as electrode, huge electric field can be induced with small driving voltage. This design enables ultraefficient electro-optic (EO) interaction within EO polymer infiltrated slot. To effectively couple light into slow light region, a PC taper from W1.08 to W1.0 is designed to minimize the group index mismatch between strip waveguide and slow light PC waveguide,[15] as shown in Fig. 1.

The hybrid nanophotonic modulator is fabricated on a silicon-on-insulator (SOI) wafer with 230 nm lightly doped top silicon and 3 μm buried oxide. Details of fabrication are described in Ref. 15. Figure 3(a) shows the fabricated MZI structure with gold electrodes. Figure 3(b) shows scanning electronic microscopy (SEM) image of the silicon PC slot waveguide. The EO polymer was processed using standard methods[16] and poled with high electric field of 200 V/μm. Figure 3(c) shows cross sectional view of the 75 nm slot infiltrated with EO polymer. Compared to other devices with slot width over 120 nm,[10,17] our narrower slot will provide higher modulation efficiency at same driving voltage.

To characterize the modulator performance, transverse electric light from a broadband source was butt coupled into the modulator with a polarization maintaining tapered lensed fiber. Transmitted light was collected by a single mode lensed fiber and analyzed with an optical spectrum analyzer. We observe a 5 nm deviation in the photonic band edge at 1569 nm compared to simulation results, which is attributed to fabrication errors. A laser source was tuned to 1564.5 nm, corresponding to the slow light region, where maximum modulation response is achieved. The modulator was biased at 3 dB point and driven by a 50 KHz triangular wave. Modulated optical signal was converted to electrical signal through a gain-switchable photodetector. Figure 4 shows that the EO polymer nanophotonic modulator has a V_π of 1.8 V. The effective EO coefficient is defined as $\gamma_{33}=\lambda w/n^3 V_\pi \Gamma L=1565\times 75\ \text{nm}^2/1.63^3\times 1.8\ \text{V}\times 0.37\times 308\ \mu\text{m}=132\ \text{pm/V}$, where Γ is the fraction of the total power in the slot. The value of $\Gamma=0.37$ is given by simulation results in Fig. 2(b). The device also achieves very high modulation efficiency $V_\pi\times L=1.8\ \text{V}\times 308\ \mu\text{m}=0.56$ V mm. This result is nearly one order of magnitude lower than that reported in Ref. 9.

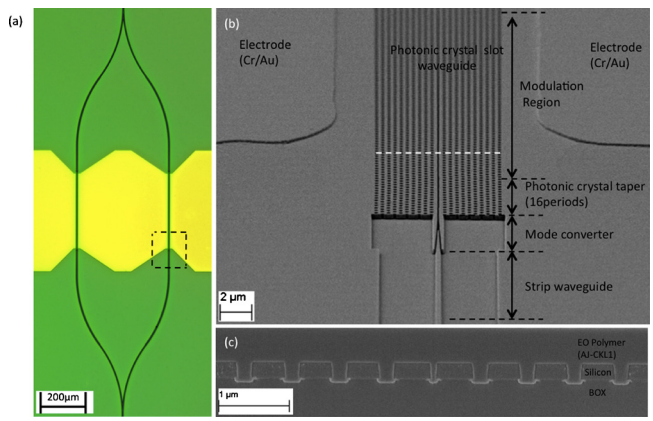

FIG. 3. (Color online) (a) Optical microscope picture of the fabricated MZM structure. (b) SEMs picture showing the enlarged view of the dotted square area in (a). (c) Cross-sectional SEM picture take across the dotted line in (b) after covering the entire structure in (a) with AJ-CKL1/APC. Complete infiltration of EO polymer into the 217 nm air holes and 75 nm slot is confirmed.

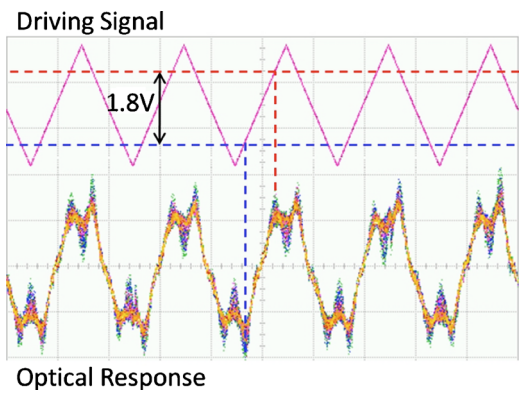

FIG. 4. (Color online) Low frequency modulation transfer-function measurement at 1564.5 nm wavelength: upper, applied voltage; lower, optical output signal. The half-wave voltage V_π is determined by finding the difference between the applied voltage at which the optical output is at a maximum and the voltage at which the optical output is at the next minimum.

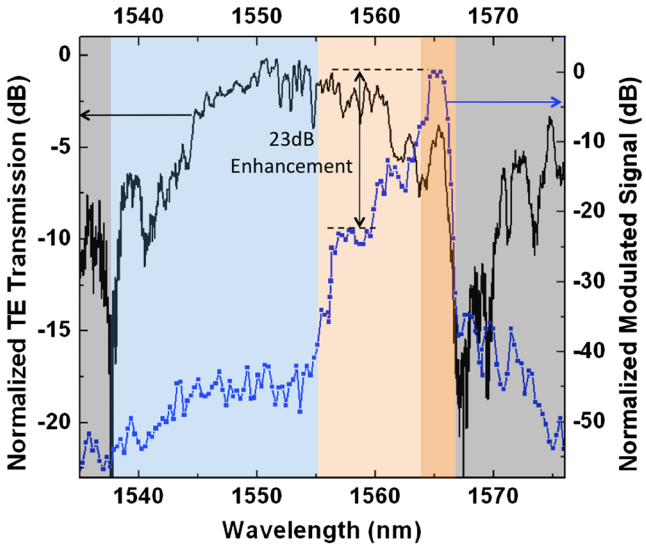

FIG. 5. (Color online) Wavelength dependence of normalized modulated signal (blue) and normalized optical transmission (black). Four distinct regions are shown in this figure: normal group velocity region with high optical transmission and low modulated signal (blue); transitional region with gradually decreased optical transmission and rapidly increased modulated signal (light orange); slow light region with relatively low optical transmission but extremely high E-O modulation (orange); photonic band gap and beyond with minimized modulation (gray).

To confirm the dramatic EO modulation enhancement out of slow light effect, all testing conditions were fixed and wavelength tuned from 1535 to 1575 nm. The wavelength dependence of normalized modulated signal under 1 V of driving voltage is plotted in Fig. 5, together with normalized optical transmission spectrum of the EO polymer nanophotonic modulator. The defect-guided mode of PC slot waveguide occurs from 1538 to 1567 nm. Although optical transmission reaches maximum at ~1550 nm, the normalized modulated signal is only about −45 dB. As we tune to longer wavelength (transitional region in Fig. 5), intensity of the modulated signal increases dramatically due to slow light enhancement. The peak modulated signal around 1565 nm is 23 dB higher than in transitional region, where the photodetector starts to measure sensible modulation response. Above 1566 nm, modulated signal decreases sharply due to transmission cut-off by photonic band gap.

In summary, we achieved 23 dB modulation enhancement of EO polymer nanophotonic modulator from slow light effect. The low $V_{\pi} \times L$ of 0.56 V mm represents the best figure of merit achieved for EO polymer modulator. Such compact and highly efficient nanophotonic modulator is an ideal candidate for on-chip optical interconnects. It should be noted that efficiency from poled EO polymer materials in silicon nanoslot is still lower compared to the best results obtained from poling of thin films. Solving issues related to high electric field poling of EO polymer in silicon could lead to ultracompact devices with extremely low power operation for applications in dense wavelength-division multiplexing, phased array antennas, and photonic analog-to-digital converters.

This work was supported by AFOSR STTR program (Grant No. FA9550-09-C-0086), monitored by Dr. Charles Y.-C. Lee.

[1]Q. Xu, B. Schmidt, S. Pradhan, and M. Lipson, Nature (London) **435**, 325 (2005).
[2]A. Liu, R. Jones, L. Liao, D. Samara-Rubio, D. Rubin, O. Cohen, R. Nicolaescu, and M. Paniccia, Nature (London) **427**, 615 (2004).
[3]T. Gray, T.-D. Kim, D. B. Knorr, J. Luo, A. K. Y. Jen, and R. M. Overney, Nano Lett. **8**, 754 (2008).
[4]M. Lee, H. E. Katz, C. Erben, D. M. Gill, P. Gopalan, J. D. Heber, and D. J. McGee, Science **298**, 1401 (2002).
[5]D. Chen, H. R. Fetterman, A. Chen, W. H. Steier, L. R. Dalton, W. Wang, and Y. Shi, Appl. Phys. Lett. **70**, 3335 (1997).
[6]Y. Enami, C. T. Derose, D. Mathine, C. Loychik, C. Greenlee, R. A. Norwood, T. D. Kim, J. Luo, Y. Tian, A. K. Y. Jen, and N. Peyghambarian, Nat. Photonics **1**, 180 (2007).
[7]Y. Enami, D. Mathine, C. T. DeRose, R. A. Norwood, J. Luo, A. K. Y. Jen, and N. Peyghambarian, Appl. Phys. Lett. **91**, 093505 (2007).
[8]Y. Jiang, W. Jiang, L. Gu, X. Chen, and R. T. Chen, Appl. Phys. Lett. **87**, 221105 (2005).
[9]D. M. Beggs, T. P. White, L. O'Faolain, and T. F. Krauss, Opt. Lett. **33**, 147 (2008).
[10]T. Baehr-Jones, B. Penkov, J. Huang, P. Sullivan, J. Davies, J. Takayesu, J. Luo, T.-D. Kim, L. Dalton, A. Jen, M. Hochberg, and A. Scherer, Appl. Phys. Lett. **92**, 163303 (2008).
[11]X. Chen, A. X. Wang, S. Chakravarty, and R. T. Chen, IEEE J. Sel. Top. Quantum Electron. **15**, 1506 (2009).
[12]Z. Wang, N. Zhu, Y. Tang, L. Wosinski, D. Dai, and S. He, Opt. Lett. **34**, 1498 (2009).
[13]H. Chen, B. Chen, D. Huang, D. Jin, J. Luo, A. K. Y. Jen, and R. Dinu, Appl. Phys. Lett. **93**, 043507 (2008).
[14]M. R. Patterson, S. Hughes, S. Schulz, D. M. Beggs, T. P. White, L. O'Faolain, and T. F. Krauss, Phys. Rev. B **80**, 195305 (2009).
[15]P. Pottier, M. Gnan, and R. M. De La Rue, Opt. Express **15**, 6569 (2007).
[16]C.-Y. Lin, B. Lee, A. X. Wang, W.-C. Lai, S. Chakravarty, Y. Liu, D. Kwong, R. T. Chen, J. Luo, and A. K. Y. Jen, Proc. SPIE **7607**, 76070D (2010).
[17]J. H. Wülbern, J. Hampe, A. Petrov, M. Eich, J. Luo, A. K. Y. Jen, A. Di Falco, T. F. Krauss, and J. Bruns, Appl. Phys. Lett. **94**, 241107 (2009).